Benefits of geosynthetic reinforcement in widening of embankments subjected to foundation differential settlement

L. Miao[1], F. Wang[2], J. Han[3] and W. Lv[4]

[1]*Professor, Institute of Geotechnical Engineering, Southeast University, Nanjing, Jiangsu, China, 210096, Telephone: +86 25 83795836; Telefax: +86 25 83795836; E-mail: lc.miao@seu.edu.cn (corresponding author)*
[2]*Lecturer, Institute of Geotechnical Engineering, Southeast University, Nanjing, Jiangsu, China, 210096, Telephone: +86 25 83792776; Telefax: +86 25 83795836; E-mail: feiwangseu@gmail.com*
[3]*Professor, Department of Civil, Environmental, and Architectural Engineering, University of Kansas, Lawrence, KS 66045, USA, Telephone: +1 785 864 3714; Telefax: +1 785 864 5631; E-mail: jiehan@ku.edu*
[4]*Lecturer, School of Civil Engineering, Nanjing Forestry University, Nanjing, Jiangsu 210037, China,Telephone: +86 25 85428890; Telefax: +86 25 85427768; E-mail: lvweihua@yahoo.com.cn*

Received 14 December 2013, revised 27 June 2014, accepted 9 August 2014

ABSTRACT: In the present study, physical model tests were conducted to investigate the effect of the geogrid reinforcement on the reduction of the differential settlement in widening of a highway embankment. A water bag filled with water and placed beneath an embankment was used to simulate the soft foundation of the widened portion of the embankment in the physical model test. Water from the water bag was drained to simulate the development of differential settlements between the existing and widened foundations of the embankment. The geogrid layers were installed with one side fixed in the existing embankment to provide enough anchorage in the physical model tests. Settlements of the embankment, strains in the geogrids and earth pressures were monitored during the test. The test results show that the geogrid layers stabilised the soil arching in the embankment, reduced the differential settlement on the embankment surface, and enhanced the serviceability of the widened embankment. The differential settlement reduction by geogrid reinforcement in the model tests was about 20 to 30 mm. Finally, the benefits of the geogrid reinforcement in the Jiang-Liu highway widening project including controlling the differential settlement in the embankment were validated based on the observed data.

KEYWORDS Geosynthetics, Differential settlement, Widening embankment**,** Geogrid reinforcement, Soil arching.

REFERENCE: Miao, L., Wang, F., Han, J. and Lv, W. (2014). Benefits of geosynthetic reinforcement in widening of embankments subjected to foundation differential settlement. *Geosynthetics International*, **21**, No. 5, 321–332. [http://dx.doi.org/10.1680/gein.14.00019]

1. INTRODUCTION

With the rapid economic development in China in recent decades, traffic volumes on a number of highways have approached or exceeded their design capacities. Therefore, widening of these highways is necessary and/or planned. It has been reported that over ten major highway widening projects were completed in China between 1997 and 2007 (Zhang 2007). The most challenging problem that geotechnical engineers have faced in the design of highway embankment widening is the differential settlement between existing and widened portions of an embankment. This differential settlement is mainly caused by different degrees of consolidation of soil layers under the existing and widened portions of the embankment, especially in soft soil areas.

Various types of technologies have been adopted to control the differential settlement induced by widening of highway embankments; for example, pile foundations, lightweight fill, composite foundations by columns, geosynthetic reinforcement, and a combination of above techniques. Ludlow *et al.* (1992) pointed out that the reduction of differential settlement depends on the type, tensile stiffness, and number of layers of geosynthetics. Forsman and Uotinen (1999) found that the use of geosynthetic

reinforcement could minimise the horizontal displacement of the embankment and thus prevent the development of cracks on pavements. van Meurs *et al.* (1999) performed a field study to evaluate the effectiveness of a gap-method. In this method, the widened portion of the embankment is filled starting from outside, a gap is formed and maintained between the existing and widened portions of the embankment, and the gap is filled after the consolidation of the soft soils beneath the widened embankment reach a certain level.

Geosynthetic reinforcement including geogrids, woven geotextiles, and geocells have been used for roads (Berg *et al.* 2000; Han *et al.* 2011), walls (Bathurst *et al.* 2002; Leshchinsky and Han 2004; Huang *et al.* 2009a; Allen and Bathurst 2014) and embankments (Han and Gabr 2002). Li and Gong (2001) used geogrids with gravel cushions to enhance the integrity of the existing and widened portions of the embankment. Corbet *et al.* (2002) investigated the performance of geogrid-reinforced slopes of the widened embankment through field observations. Habib *et al.* (2002) verified the performance of geosynthetic-reinforced, pile-supported widened embankments. In the recent years, more research has been devoted to the geosynthetic reinforcement in embankment widening. However, the mechanism of the geosynthetic reinforcement in mitigating the differential settlement between existing and widened portions of the embankment is not well understood and the benefits of geosynthetic reinforcement cannot be properly quantified. In several widening projects in China, different layers of geosynthetic reinforcement were installed at different elevations (Gao 2006). Han *et al.* (2007) used a numerical method to investigate stresses and deformations of the widened embankments over soft soils with and without foundation columns. They provided the recommendations for design of foundation columns for embankment widening. Even though geosynthetic reinforcement has been increasingly used in highway widening projects, the design of geosynthetic reinforcement is mostly based on the experience and judgment of designers. This situation is attributed to insufficient understanding of the mechanism of geosynthetic reinforcement in highway widening.

In the present study. physical model tests were conducted to investigate the benefits of geosynthetic reinforcement in embankment widening. In the physical model, the differential settlement between the existing and widened portions of the embankment was simulated by a water bag at different stages of water release. One or two layers of geogrid were installed within the embankment. When one layer of geogrid was used, it was placed at the bottom of the embankment. When two layers of geogrid were used, one geogrid was placed immediately above the water bag (i.e. at the bottom of the embankment) and the other was placed in the upper portion of the embankment. Water in the water bag was drained gradually to simulate the development of the differential settlement. During this process, the tensile forces in the geogrids and the settlements at different elevations were monitored. At the end, the benefits of the geogrid reinforcement in highway widening including controlling the differential settlement and improving the load distribution in the embankment were validated using the observation data from a real project. The present study investigated the embankment surface settlement induced by the differential settlement of the foundation under the widened portion. The possible settlement induced by traffic loading was not considered or investigated.

2. PHYSICAL MODEL TEST

2.1. Materials used

2.1.1. *Soil*

The soil used was taken from a construction site at the Jiang-Liu highway widening project. The properties of the soil for the physical model tests are listed in Table 1. According to the Unified Soil Classification System (ASTM D 2487), this soil was classified as CL. The moist unit weight of the soil at a moisture content of 15.2% was 18 kN/m^3 for the model test.

2.1.2. *Geogrid*

A polyester geogrid was used as geosynthetic reinforcement in this study. Considering the relatively small height of the embankment in the physical model test, uniaxial geogrid with low tensile stiffness was adopted to obtain more obvious strains in the geogrid. Figure 1 shows three tensile test results for the geogrid used in the present study and the geogrid had an ultimate tensile strength of approximately 42 kN/m. The calibration factor of the geogrid was 1.0, based on the strain gauge measurement on the geogrid when the global strain was smaller than 3%, and would be 1.05 when the global strain of the geogrid was 4%. Allen and Bathurst (2014) reported the calibration factors for high-density polyethylene geogrids ranging from 1.0 to 1.7 (the stiffer geogrid had a lower factor). Based on the test results, the average tensile stiffness of the geogrid used in the physical model test was approximately 500 kN/m. The thickness of the geogrid sheet was 1.5 mm and its elastic modulus was

Table 1. Physical properties of fill

Specific gravity, G_s	Liquid limit, LL (%)	Plastic limit, PL (%)	Plasticity index, PI (%)	Maximum dry density, γ_{dmax} (g/cm^3)	Optimum water content, w_{opt} (%)	Gradation (%)		
						$>$ 0.05 mm	0.05~0.005 mm	$<$ 0.005 mm
2.64	40.8	20.3	20.5	1.85	16.2	35.6	48.9	15.5

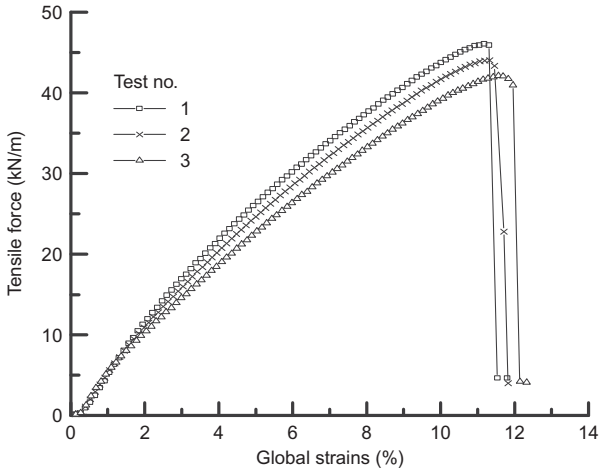

Figure 1. Geogrid tensile strength test results

0.33 GPa. The aperture of the geogrid was rectangular with dimensions of 35 mm long and 10 mm wide.

2.2. Test preparation

2.2.1. *Water bag and its calibration*

To simulate the differential settlement between the existing and widened portions of the embankment, a custom-made soft rubber water bag was used, which had a dimension of 1 m wide, 1.6 m long, and 0.3 m high as shown in Figure 2. The width of the water bag was smaller than the width of the widening embankment so that the slope failure of the widened embankment due to settlement could be prevented. The water bag was filled with water and installed beneath the widened portion of the embankment, and gradual drainage of the water in the water bag was used to simulate the development of differential settlement between the existing and widened portions of the embankment. The rate of water flow out of the water bag was controlled by a flow control valve during testing to model the differential settlement by draining water. To obtain the relationship between the subsidence of the water bag and the mass of drained water, a calibration test was performed so that the settlement at the base of the embankment could be estimated by the measured mass of the drained water. Three dial gauges were used in the calibration test to obtain the average subsidence of the water bag. Figure 3 shows the relationship between the mass of drained water and the subsidence of the water bag. The vertical load on the water bag was provided by the steel blocks. Figure 3 shows that the relationship between the mass of drained water and the subsidence of the water bag was nearly linear; therefore, the subsidence of the water bag could be easily estimated with the measured mass of drained water.

Figure 2. Photograph of the water bag

2.2.2. *Instrumentation*

Three important parameters were measured in the physical model test: the settlements and earth pressures at different elevations of the embankment, and the strains in the geogrids. Settlement plates were used to measure the settlements. These settlement plates were made of plexiglass plate, which can minimise the measured error caused by the weight of the settlement plate. The plate was square and had a width of 80 mm. A rod with a diameter of 10 mm was connected to the plate on each end. The measurement accuracy of settlement was ±0.01 mm. The strains in the geogrids were measured using resistance-type strain gauges, which were recorded automatically by a computer in real time. The accuracy of the strain gauge was ±0.1 με. In order to investigate the stress state change caused by the different settlement in the fill embankment, vertical earth pressures were measured by earth pressure cells. The earth pressure cells (20 mm in diameter and 7 mm in thickness) were used to measure the earth pressures at different elevations in the embankment. The vertical earth pressure data were used to evaluate soil arching effect during the development of the differential settlement. The accuracy of the earth pressure cell is ±1 Pa. Before installation of the earth pressure cells, they

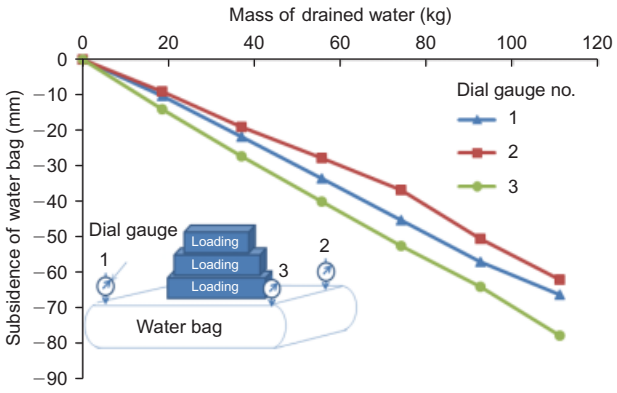

Figure 3. Relation of the mass of water released and the water bag subsidence

were calibrated using the air pressure calibration method to obtain the following relationship

$$y = kx \quad (1)$$

where x is the measured strain of the earth pressure cell under air pressure, y is the corresponding pressure, and k is the calibration factor.

2.3. Physical model testing

2.3.1. *Physical model pit and construction*

A model test pit made of concrete was constructed. The pit was 4.15 m long, 1.60 m wide and 0.9 m high. Assuming the symmetry of the model, only half of the model was constructed. The existing embankment had a dimension of 1.00 m wide on the crest and 1.65 m long. All of the physical model tests were done under normal gravity (i.e. 1*g*) condition. Figure 4 shows the three-dimensional view of the physical model. The side slope of the embankment before and after widening was 1.5:1 (H:V). A 1.5 m wide and 0.3 m high brick layer was used to simulate a fully-consolidated foundation (assuming no additional settlement would happen during and after widening) under the existing portion of the embankment. The water bag was installed adjacent to the brick layer to simulate the differential settlement between the foundations under the existing and widened portions of the embankment. Deformations of the existing and widened portions of the embankment during construction were neglected. To place the existing and widened portions of the embankment conveniently, the upper surface of the brick layer had the same elevation as the top of the water bag, and the existing and widened portions were constructed simultaneously.

The soil taken from a construction site was first air-dried and then crushed and mixed with water to achieve the optimum moisture content obtained in the standard Proctor tests (ASTM D 698). In order to study the reinforcement effect of geogrid(s) within the embankment, three physical model tests were conducted, namely (1) a widened embankment without any geogrid, (2) a widened embankment with a single geogrid, and (3) a widened embankment with two geogrid layers. The process of embankment construction for these three cases is described below. For the widened embankment without any geogrid as shown in Figure 5(a), the embankment was directly filled on the top of the brick stage and the water bag in lifts up to the design elevation. For the widened embankment with a single geogrid as shown in Figure 5(b), a 50 mm thick soil layer was first placed on the top of the brick stage and the water bag and then a geogrid was installed and fixed by U iron nails at the

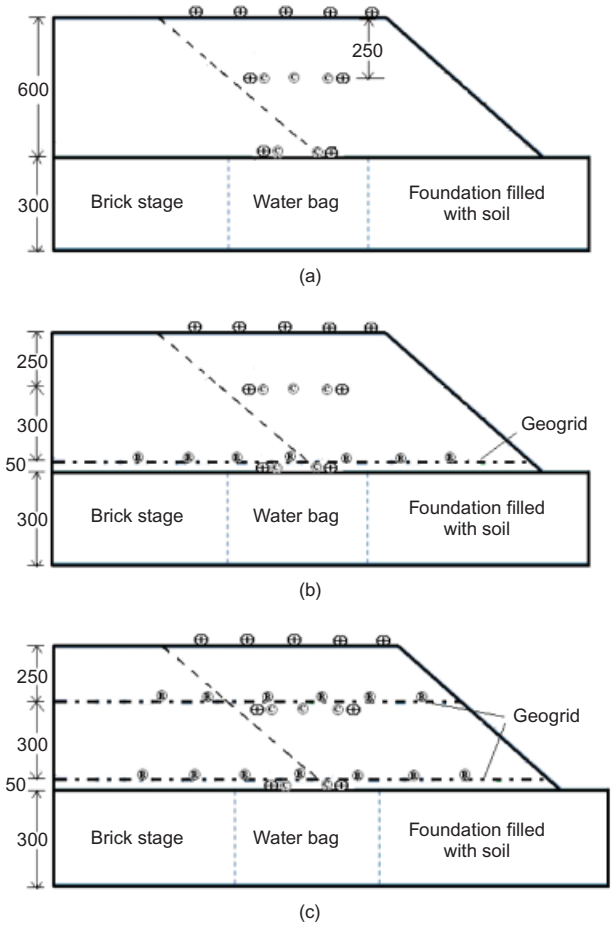

Figure 5. Diagrammatic sketches of widened embankment for physical model tests (unit: mm) (not to scale): (a) widened embankment without any geogrid; (b) widened embankment with a single geogrid; (c) widened embankment with two geogrids. Symbols: ⊕: settlement measurement, Ⓒ: earth pressure cell, Ⓡ: strain gauges

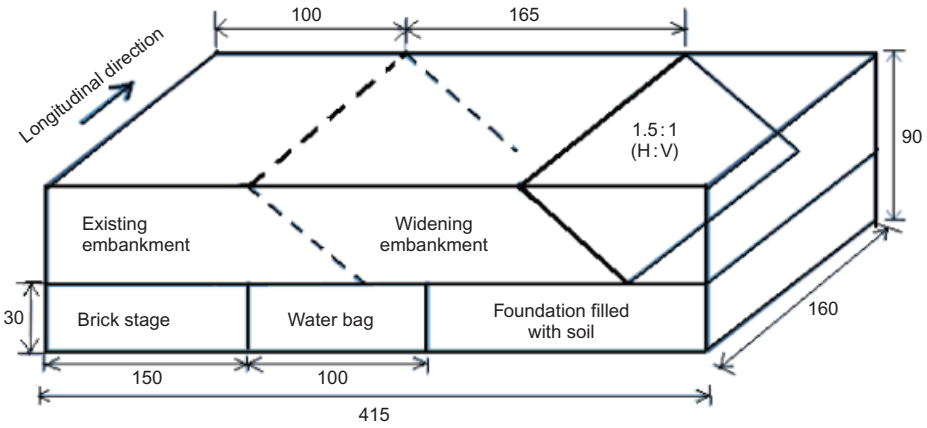

Figure 4. Configuration of the physical model (unit: cm) (not to scale)

existing embankment with an overlap length of 500 mm. The fixing of the geogrid is necessary to ensure the geogrid to provide enough anchorage. The soils were filled in lifts up to the design elevation. For the widened embankment with two geogrid layers as shown in Figure 5(c), the initial procedure for the model construction was the same as that in the last test. After the first geogrid layer was installed, the embankment was then filled with the soil in three lifts with each lift thickness of 100 mm. The second geogrid layer was subsequently installed and also fixed by U iron nails at the existing embankment with the overlap length of 500 mm. At the end, the embankment was filled in two lifts with each lift thickness of 125 mm to the surface of the embankment. The locations of these two geogrid layers were determined based on the numerical simulation results prior to the model tests. All the measurement devices were installed during the construction of the embankment, and the initial data was measured for all the devices after the completion of the construction of the embankment. Additional tests are needed to investigate the optimum location of geogrid layers, which will be investigated in a future study.

It should be noted that the model test has some limitations. For example, the water bag in the laboratory study had a whole block settlement; however, in field, the settlement of an embankment foundation has a settlement basin. In field, the settlement of an embankment foundation involves a consolidation process under not only an embankment load but also a traffic load. The model tests in the present study only simulated the widened embankment subjected to foundation settlement and no traffic loading was considered.

2.3.2. *Instrumentation*

In total, nine settlement plates were installed at three elevations: namely five settlement plates on the embankment surface, two settlement plates at a depth of 250 mm from the embankment surface (i.e. immediately below the upper geogrid layer if two geogrid layers were used), and two settlement plates immediately above the water bag. The locations of the settlement plates are shown in Figure 5. Strain gauges were installed on the geogrid layers. On each geogrid layer, one row of strain gauges was placed at the centreline of the pit in the width direction. Five earth pressure cells were installed at two elevations: three cells were at the mid-depth of the embankment (immediately below the upper geogrid layer) and two cells were immediately above the water bag. Figure 5 shows the locations of the earth pressure cells.

2.4. Water draining plan

To simulate the development of the differential settlement, 12 stages of water draining were planned. Within each stage, a desired quantity of water drained out of the bag. The complete water-draining plan is summarised in Table 2. An electric scale was used to measure the weight of the drained water in real time. If a desired weight was reached, the valve was closed until the measured settlements, strains, and earth pressures became constant and then the next water draining stage started.

3. TEST RESULTS AND ANALYSIS

3.1. Settlement

Figures 6 to 8 present the measured settlements on the embankment surface at 48 h after the end of water draining for three widened embankment model tests, respectively. The test results clearly show that the settlement increased with the amount of drained water (i.e. the water bag subsidence). Figure 6 shows the maximum settlements on the embankment surface because the widened embankment was not reinforced by a geogrid.

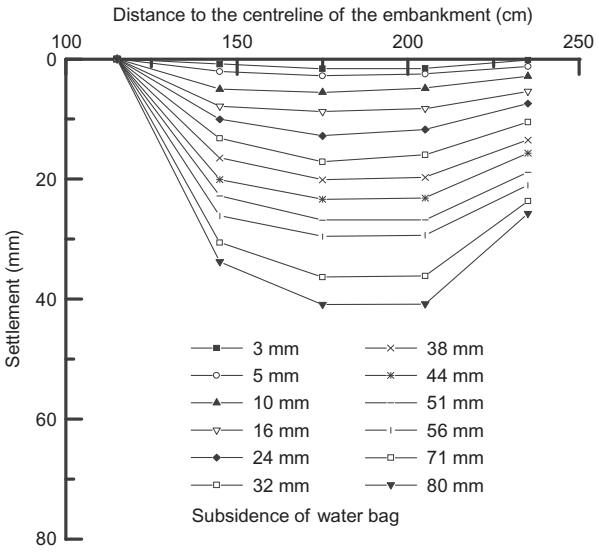

Figure 6. Settlement on the embankment surface for widening embankment with no geogrid

Table 2. Water draining plan

Water draining stages no.	Desired total mass of the released water (kg)	Corresponding subsidence of water bag (mm)	Water draining stages no.	Desired total mass of the released water (kg)	Corresponding subsidence of water bag (mm)
1	5	3	7	47	38
2	8	5	8	57	44
3	13	10	9	69	51
4	20	16	10	76	56
5	30	24	11	104	71
6	40	32	12	121	80

Note: the desired total weight is the accumulated weight of the drained water from the previous stages.

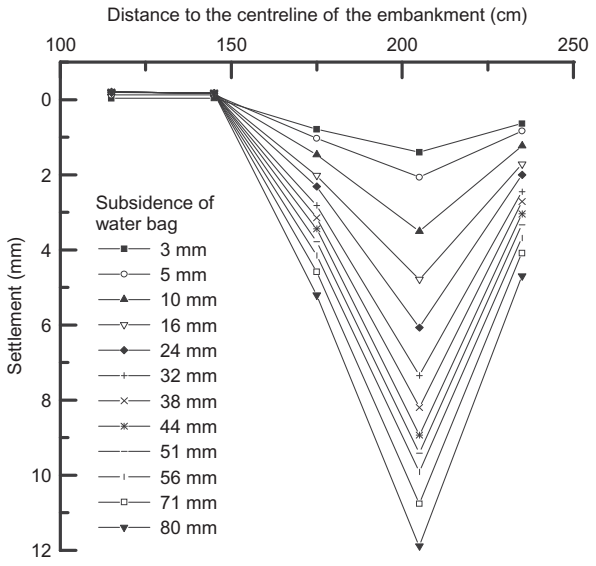

Figure 7. Settlement on the embankment surface for widening embankment with single geogrid layer

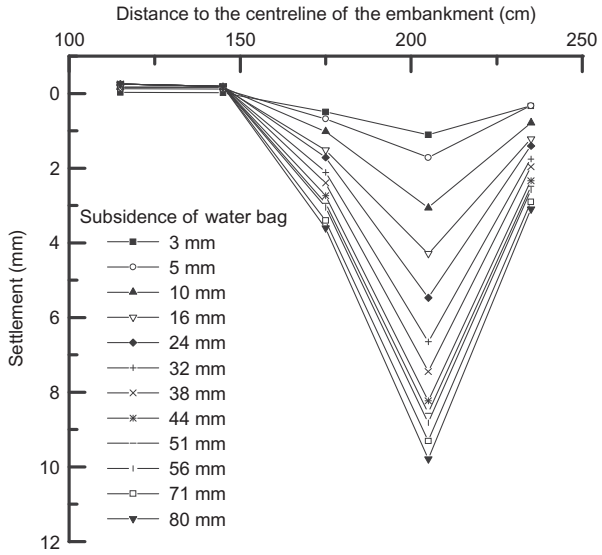

Figure 8. Settlement on the embankment surface for widening embankment with two geogrid layers

Obvious differential settlement occurred between the existing and widened portions of the embankment. It can be seen in Figure 7 that the settlements on the embankment surface were clearly reduced by the single geogrid in comparison with the unreinforced case. The geogrid had an obvious tensioned membrane effect to minimise the differential settlement when the subsidence induced by the draining of the water bag increased. Figure 8 shows that two geogrid layers slightly reduced the settlements on the embankment surface of the widened embankment in comparison with those with a single geogrid layer. The test results also show that the tensioned membrane effect of the second geogrid layer was obviously reduced. The settlement ratio (defined as the ratio of the maximum settlement on the embankment surface to the water bag subsidence) decreased initially with the increase of water bag subsidence (Figure 9). The rate of settlement ratio

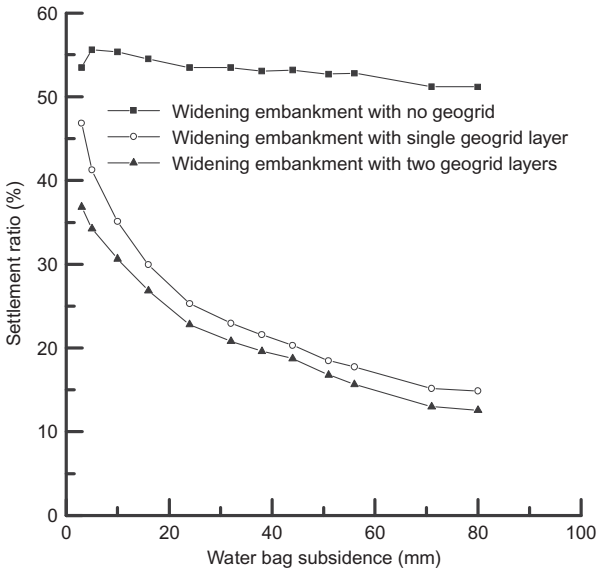

Figure 9. Variation of settlement ratio on the surface of the embankment with the subsidence of water bag

variation decreased after the water bag subsidence became greater than 70 mm. Figure 9 also shows that the settlement ratio of the widened embankment without any geogrid was a maximum. The settlement ratio of the widened embankment with a single geogrid layer was slightly larger than that of the widened embankment with two geogrid layers. The effect of the upper geogrid in controlling the different settlement was less than that of the lower geogrid because a smaller differential settlement occurred at the higher elevation. The above discussion demonstrates that the geogrid can be used to control the differential settlement of a widened embankment. According to British Standard BS 8006 (BSI 2011), it is beneficial to install multiple layers of geogrid to mitigate the differential settlement in highway projects for embankment widening. However, an increase of geogrid layers increases the cost. A balance has to be sought between the reduced differential settlement and the economy for actual projects.

3.2. Strain in the geogrid

Figure 10 presents the strain distributions along the geogrids for the widened embankment with a single geogrid layer at 48 h after the end of water draining. The strains reported in this and later figures are local strains. As the calibration factor is 1.0, they also represent the global strains. Two peak strains were found in the strain distribution of the geogrid layer, in which the peak strain adjacent to the fixed side of the geogrid was slightly greater than that close to the free side, but the two peaks became less obvious as the subsidence of the water bag increased.

The measured strain distributions along the lower geogrid in the widened embankment with two geogrid layers at 48 h after the end of water draining are shown in Figure 11. Two peak strains were found in the strain distributions of the lower geogrid layer. The peak strain adjacent to the fixed side of the geogrid was greater than

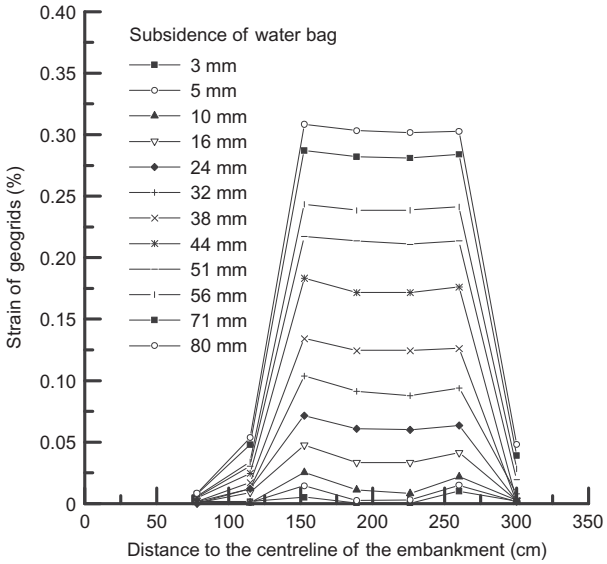

Figure 10. Strain of the geogrid at different subsidence of water bag for widening embankment with a single geogrid layer

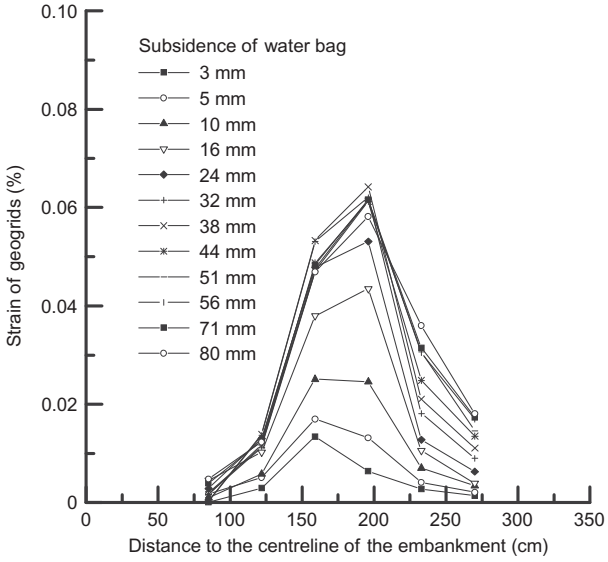

Figure 12. Strain of the second geogrid layer at different subsidence of water bag for widening embankment with two geogrid layers

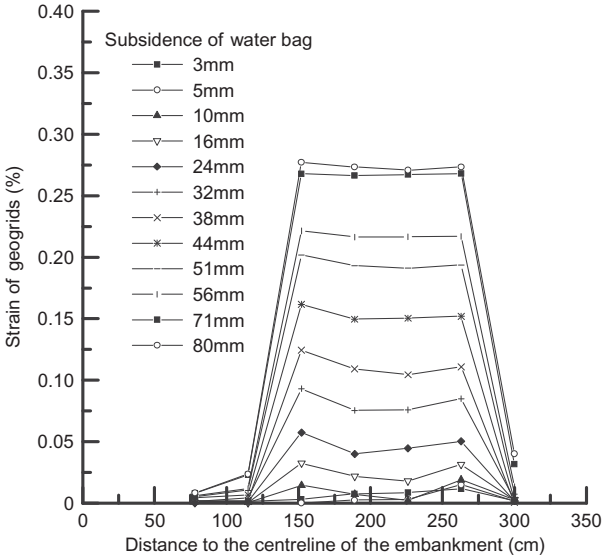

Figure 11. Strain of the first geogrid layer at different subsidence of water bag for widening embankment with two geogrid layers

that close to the free side. However, these two peak strains became stable with the time after the end of the water draining and the subsidence of the water bag increased. The possible explanation is that the tensile strain in the geogrid was redistributed with time. It is also shown that the lower geogrid layer had the peak strains at two sides of the water bag. This phenomenon is similar to that reported by Han and Gabr (2002) in a geosynthetic-reinforced, pile-supported embankment due to the stress concentration at the boundaries of the stable and moving portions of the foundation.

Figure 12 shows the strain distributions along the upper geogrid in the widened embankment with two geogrid layers at 48 h after the end of water draining. A single peak strain was found in the strain distribution of the upper geogrid layer; the reason being that the pullout resistance of the geogrid on each side was limited due to low overburden stress. However, the peak strains in the upper geogrid layer did not change significantly when the subsidence of the water bag was larger than 44 mm. This result implies that the existence of the upper geogrid layer limited the reflection of the differential settlement towards the embankment surface. This phenomenon can be verified by comparing the settlement ratio of the widened embankment with a single geogrid layer with that having two geogrid layers as shown in Figure 9. The subsidence of the water bag did not affect the settlement on the embankment surface after the water bag had subsided more than 44 mm. This result illustrates that stable soil arching was formed in the widened embankment above the upper geogrid.

3.3. Earth pressure in the embankment

The measured earth pressures as the subsidence of the water bag increased after embankment widening without any geogrid are shown in Figure 13. These earth pressures at the same elevations remained constant and were approximately equal to the overburden stresses. Figure 14 shows the measured earth pressures as the subsidence of the water bag increased after embankment widening with a single geogrid layer. The measured earth pressures on the top of the water bag decreased as the subsidence of the water bag increased, especially at the initial stage of subsidence. The earth pressures on the top of the water bag became approximately constant when the subsidence of the water bag was larger than 56 mm because the soil arching was fully formed within the embankment. The measured earth pressures with an increase of the water bag subsidence for embankment widening with two geogrid layers are presented in Figure 15. The increase of the water bag subsidence reduced the earth pressures

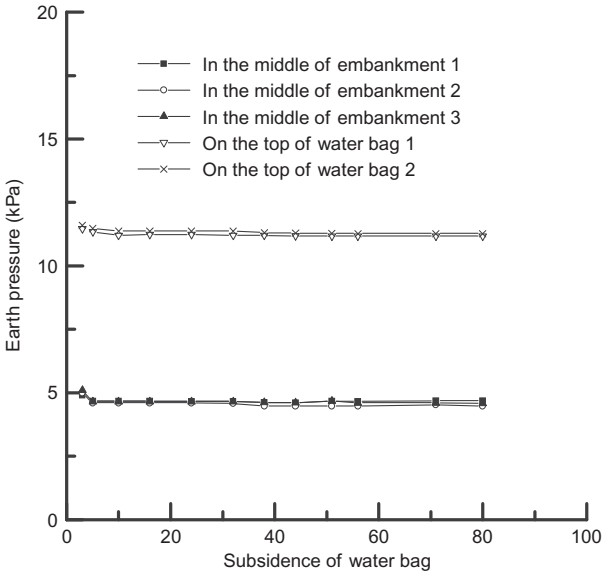

Figure 13. Measured earth pressures with the water bag subsidence for widening embankment with no geogrid

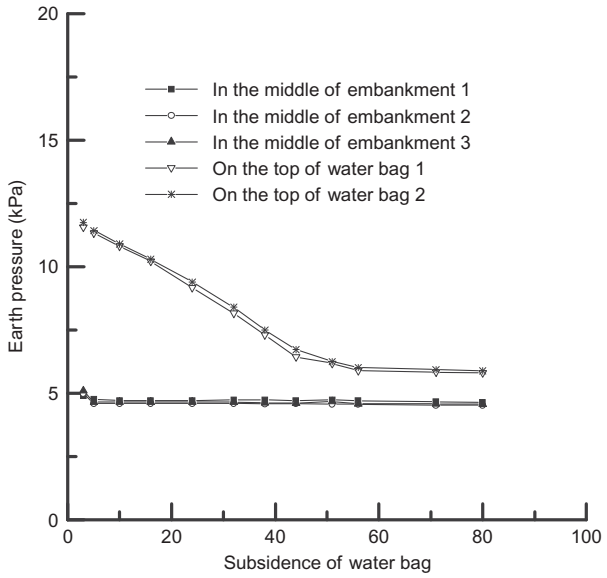

Figure 14. Measured earth pressures with the water bag subsidence for widening embankment with single geogrid layer

below both the first and second geogrid layers. They became almost constant when the water bag subsided more than 56 mm. The reduction of the earth pressure can be attributed to the soil arching effect in the embankment fill. The constant earth pressure at the large subsidence indicates stable soil arching was formed. The degree of soil arching can be evaluated by a soil arching ratio, which is defined as the ratio of the pressure measured below the geogrid to the overburden pressure of the embankment fill above the geogrid. The soil arching ratio below the lower or upper geogrid layer decreased from 1.0 (the value when the water bag had zero subsidence) to 0.4 when the water bag had subsided more than 56 mm.

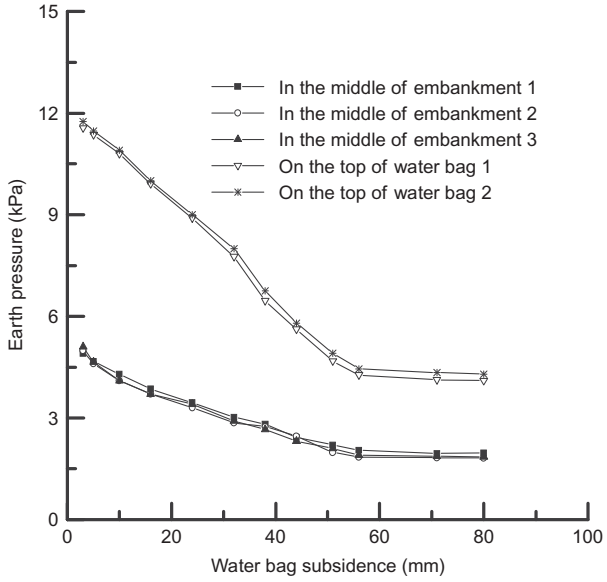

Figure 15. Measured earth pressures with the water bag subsidence for widening embankment with two geogrid layers

4. FIELD EMBANKMENT WIDENING WITH GEOGRID REINFORCEMENT

As discussed earlier, the physical model tests indicated that the existence of the geogrid layers significantly reduced the differential settlement reflected from the foundation to the embankment surface. To validate the laboratory results, a field study was conducted at the Jiang-Liu highway widening project in Yangzhou, China. In this project, the existing embankment was widened from four to eight lanes. Figure 16 shows the cone penetration test profile of the site. Controlling modulus columns (CMCs) with column caps were used to improve soft foundations, increase bearing capacity, support the widening embankment load, and reduce the total settlement. A brief description of the CMCs can be found in the paper by Miao *et al.* (2009). CMCs were installed by special equipment and made of low-strength C20 concrete. The CMCs columns were 16 m long with a diameter of 400 mm, and a spacing of m in a triangular pattern. The column caps were made of reinforced C20 concrete and had dimensions of 1400 mm × 1400 mm × 300 mm. To reduce the differential settlement between the existing and widened embankments, a uniaxial punched-drawn for high-density polyethylene geogrid layer with tensile strength of 60 kN/m was selected and installed at the bottom of the widened embankment in one test section based on the laboratory model test results as shown in Figure 17. For comparison purposes, no geogrid was used in another test section. The existing embankment was first excavated by 2 m wide, and the geogrid layer was fixed using U-shaped iron nails across the excavated portion to provide enough anchorage. Earth pressure cells were placed on top of CMC columns and soil and under the geogrid if it was used. Figure 18 shows the measured earth pressures on the column caps and soil. The measured earth pressures on the soil in the geogrid-reinforced section as shown in Figure 18(a) were lower than those in the unreinforced section in

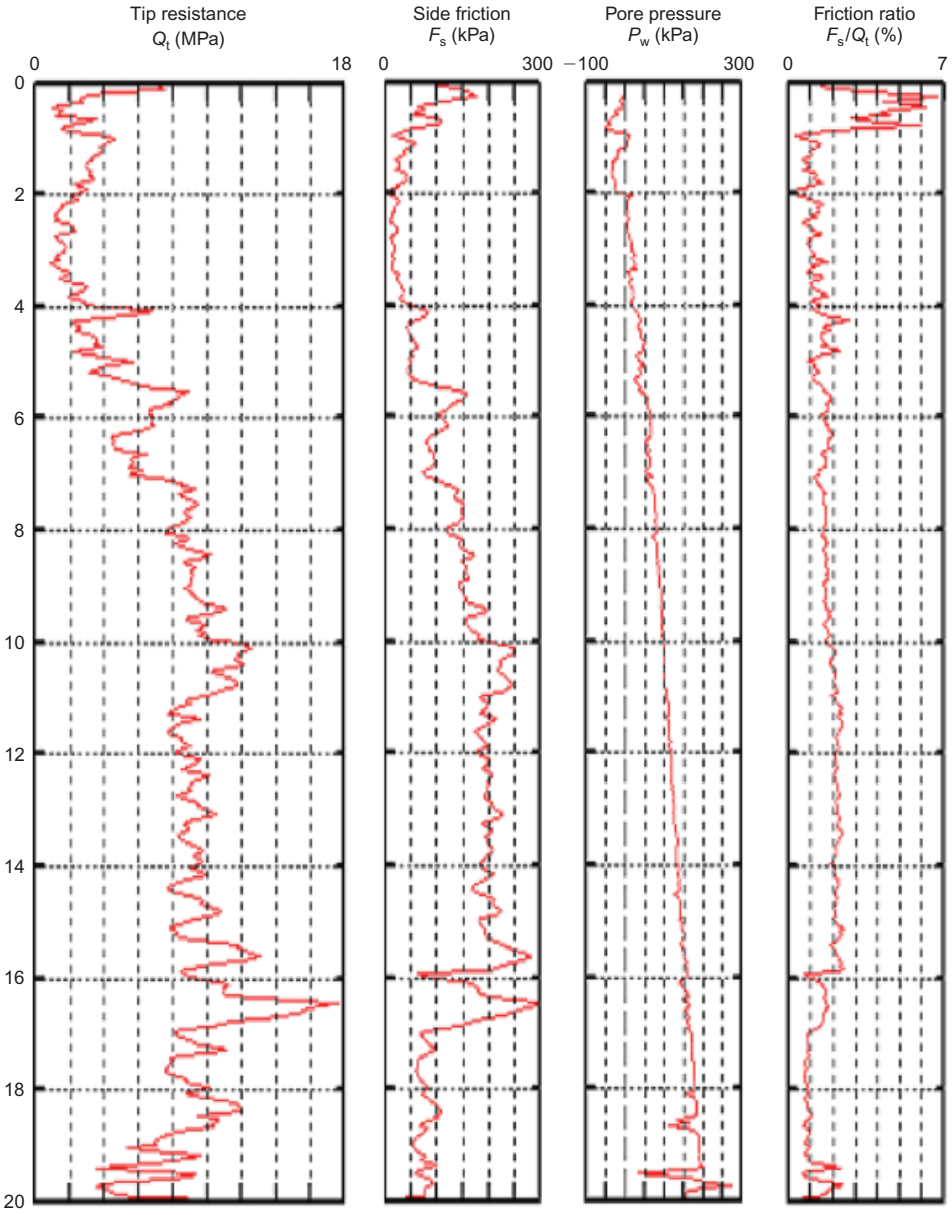

Figure 16. Cone penetration test profiles in the Jiang-Liu highway widening project

Figure 17. Photograph showing an installed geogrid under the widening embankment

Figure 18(b) because of the tensioned membrane effect in the reinforced section. Figure 19 shows the measured tensile forces in the geogrid. The maximum tensile strain in the geogrid was smaller than 1%. As a result of the increased embankment load and the soil arching effect, the measured pressures above the CMC caps increased. The measured pressures on the soil between the CMCs decreased because of the tensioned membrane effect and the load transfer from soil to column during consolidation. This phenomenon was also observed by Huang *et al.* (2009b). The measured maximum tensile force in the geogrid was located at the edge of the column caps. This result is consistent with the numerical result obtained by Han and Gabr (2002). Figure 20 shows the settlements during the construction of the widened embankment including the settlement at the bottom of the centreline of the existing embankment and widening embankments with

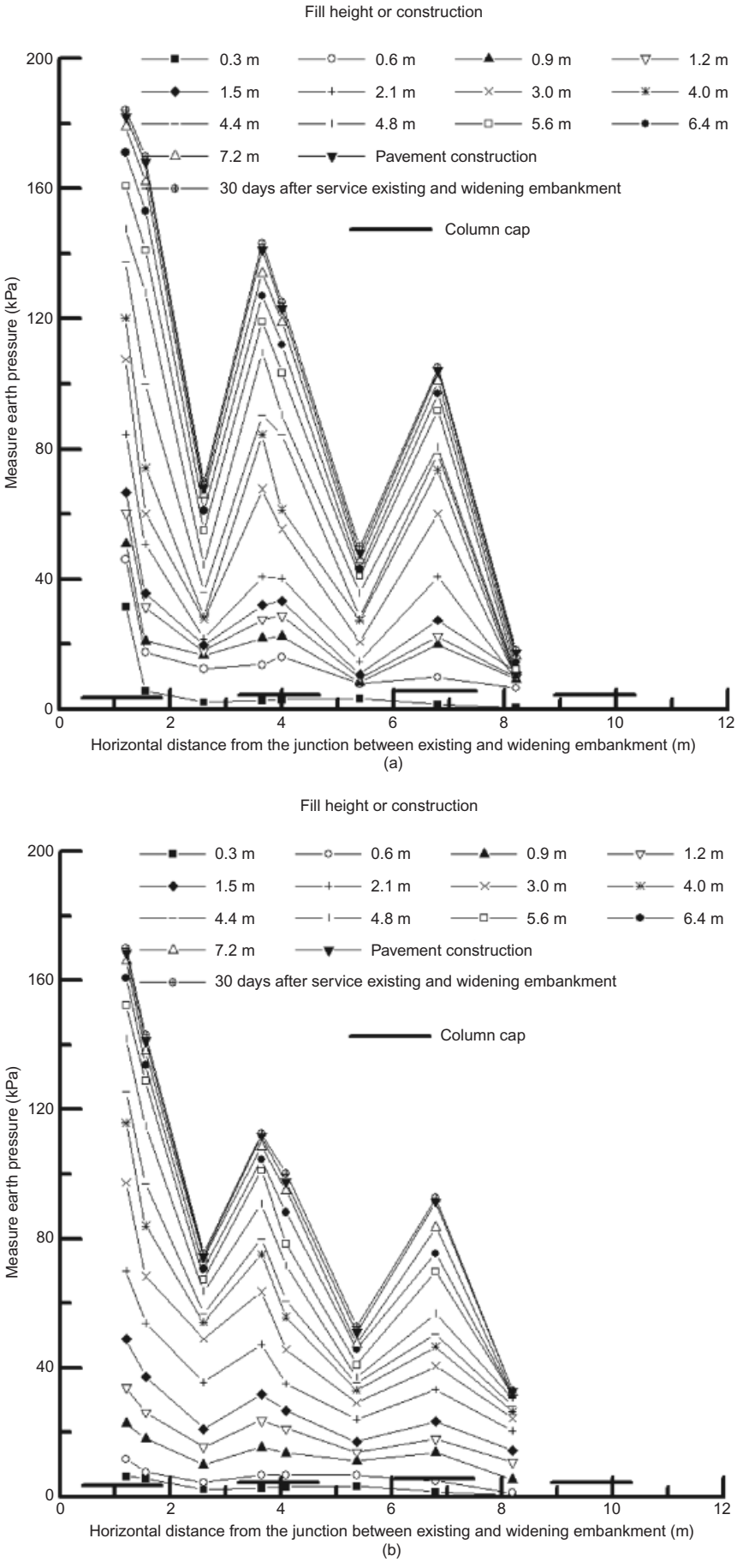

Figure 18. Measured earth pressures on column caps and soil: (a) with a geogrid; (b) without geogrid

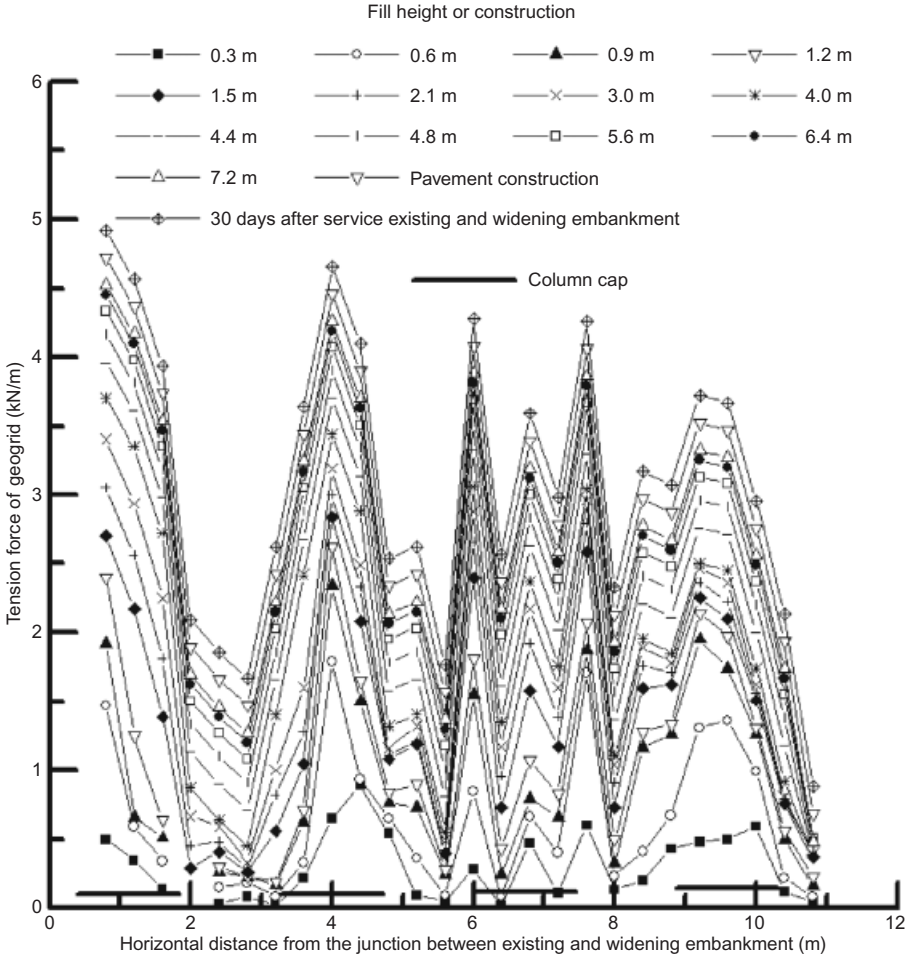

Figure 19. Measured tensile forces in the geogrids at different fill heights

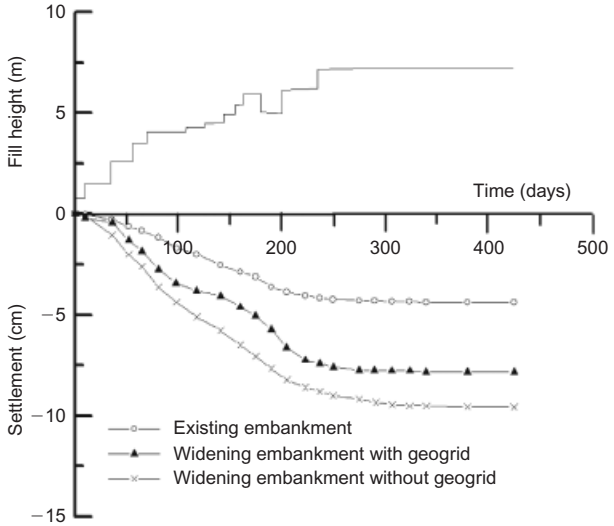

Figure 20. Measured settlements at the bottom of the embankment during the construction of the widening embankment

and without a geogrid. In this project, the settlement plates were installed at the bottom of the widening embankment with and without a geogrid along its centre of gravity (i.e. approximately 3 m away from the junction between the existing and widening embankments). The settlement plate of the existing embankment in the project was installed in the bottom of the centreline of the existing embankment during construction because it had to be conducted according to the code for Chinese highway construction (MOC 2006). The field measurements showed that the geogrid reinforcement reduced the total settlements of the widening embankment and the differential settlements between the existing and widening embankments. The settlement of the foundation under the widened embankment became stable shortly after the completion of filling the embankment. The ratio of the differential settlement to half width of the embankment crest was smaller than 0.2%, which was less than the design value of 0.5%.

5. CONCLUSIONS

Physical model tests were conducted to evaluate the benefits of the geogrid reinforcement in highway widening. A water bag with water draining at different stages was used to simulate the differential settlement between the existing and widened portions of the embankment. Settlement plates, strain gauges, and earth pressure cells were used to monitor the behaviour of the embankment during and after widening. A field test was conducted to verify the results from the physical model tests. The following conclusions can be drawn from the information obtained in the present study.

1. The settlement on the embankment surface increased with the subsidence of the foundation and time. The ratio of the surface settlement to the foundation subsidence decreased as the subsidence increased. The presence of the geogird stabilised the soil arching and minimised the settlement reflected from the foundation subsidence.
2. The settlement ratio of the embankment reinforced by geogrid became constant after the water foundation subsided more than 44 mm. This result demonstrate that the serviceability of the embankment could be ensured with appropriate geogrid reinforcement.
3. Two peak strains were measured on the lower geogrid layer near the boundaries between the stable and moving portions of the foundation. One peak strain in the upper geogrid layer was limited by the pullout resistance of the geogrid on the side close to the slope facing.
4. The measured earth pressures below both the upper and lower geogrid layers decreased with the increase of the foundation subsidence due to the soil arching effect in the embankment fill. The soil arching ratios decreased from 1.0 to 0.4 below both the upper and lower geogrid layers when the subsidence of the foundation increased from zero to a large value (56 mm herein).
5. The field study using geogrid reinforcement in the Jiang-Liu highway embankment widening project confirmed that the geogrid layer reduced the differential settlement between the existing and widened embankments.

ACKNOWLEDGEMENT

The research work presented in this paper was carried out as part of the project No. 51278099 supported by the National Natural Science Fund of China.

REFERENCES

Allen, T. M. & Bathurst, R. J. (2014). Performance of a 11 m high block-faced geogrid wall designed using the K-stiffness method. *Canadian Geotechnical Journal*, **51**, No. 1, 16–29

ASTM D 2487 *Standard Classification of Soils for Engineering Purposes (Unified Soil Classification System)*. Sec. 4, 04. 08. ASTM International, West Conshohocken, PA, USA.

ASTM D 698 *Standard Test Methods for Laboratory Compaction Characteristics of Soil using Standard Effort*. ASTM International, West Conshohocken, PA, USA.

Bathurst, R. J., Allen, T. M. & Walters, D. L. (2002). Short-term strain and deformation behavior of geosynthetic walls at working stress conditions. *Geosynthetics International*, **9**, No. 5–6, 451–482.

Berg, R. R., Christopher, B. R. & Perkins, S. W. (2000). *Geosynthetic Reinforcement of the Aggregate Base Course of Flexible Pavement Structures, GMA White Paper II*, Geosynthetic Materials Association, Roseville, MN, USA.

BSI (2011). *BS 8006–21: Code of Practice for Strengthened/Reinforced Soils and Other Fills*. BSI, London, UK.

Corbet, S. P., Rigby-Jones, J., Naylor, M. *et al.* (2002). A2/M2 widening: the use of geosynthetics for reinforced slopes. *Proceedings of the 7th International Conference on Geosynthetics*, Nice, France, September 22–27, pp. 275–278.

Forsman, J. & Uotinen, V. M. (1999). Synthetic reinforcement in the widening of a road embankment on soft ground. *Geotechnical Engineering for Transportation Infrastructure*, Barends, F. B. J., Lindenberg, J., Luger, H. J., Verruijt, A. & de Quelerij, L., Editors, CRC Press, Boca Raton, FL, USA, Vol. 3, pp. 1489–1496.

Gao, X. (2006). *Research on the Interaction between New and Existing Embankments and Treatment Techniques in Highway Widening Engineering*. PhD thesis, Southeast University, Nanjing, China (in Chinese).

Habib, H., Brugman, M. & Uilting, B. (2002). Widening of Road N247 founded on a geogrid-reinforced mattress on piles. *Proceedings of the 7th International Conference on Geosynthetics*, Nice, France, September 22–27, pp. 369–372.

Han, J. & Gabr, M. A. (2002). Numerical analysis of geosynthetics-reinforced and pile-supported earth platforms over soft soil. *Journal of Geotechnical and Geoenvironmental Engineering*, **128**, No. 1, 44–53.

Han, J., Oztoprak, S., Parsons, R. L. & Huang, J. (2007). Numerical analysis of foundation columns to support widening of embankments. *Computers and Geotechnics*, **34**, No. 6, 435–448.

Han, J., Pokharel, S. K., Yang, X., Manandhar, C., Leshchinsky, D., Halahmi, I. & Parsons, R. L. (2011). Performance of geocell-reinforced RAP bases over weak subgrade under full-scale moving wheel loads. *Journal of Materials in Civil Engineering, ASCE*, **23**, No. 11, 1525–1534.

Huang, B., Bathurst, R. J. & Hatami, K. (2009a). Numerical study of reinforced soil segmental walls using three different constitutive soil models. *Journal of Geotechnical and Geoenvironmental Engineering*, **135**, No. 10, 1486–1498.

Huang, J., Han, J. & Oztoprak, S. (2009b). Coupled mechanical and hydraulic modeling of geosynthetic-reinforced column-supported embankments. *ASCE Journal of Geotechnical and Geoenvironmental Engineering*, **135**, No. 8, 1011–1021.

Leshchinsky, D. & Han, J. (2004). Geosynthetic reinforced multitiered walls. *ASCE Journal of Geotechnical and Geoenvironmental Engineering*, **130**, No. 12, 1225–1235.

Li, S. P. & Gong, C. L. (2001). Application of geogrids with gravel cushion in a highway embankment widening project over soft soils. *Roadway*, **11**, No. 1, 20–23 (in Chinese).

Ludlow, S., Chen, W. F., Bourdeau, P. L. & Lovell, C. W. (1992). *Embankment Widening and Grade Raising on Soft Foundation*. Purdue University, West Lafayette, IN, USA, FHWA-IN-JHRP-91–18.

Miao, L. C., Wang, F., Zhang, Y. J. & Zhang, C. X. (2009). Experimental study on controlled modulus column methods. *Advances in Ground Improvement*, Han, J., Zheng, G., Schaefer, V. R. & Huang, M. S., Editors, ASCE, Reston, VA, USA, Geotechnical Special Publication no. 188, pp. 112–119.

MOC (Ministry of Communications of the People's Republic of China) (2006). *JTG F10-2006: Technical Specification for Construction of Highway Subgrades*. MOC, Beijing, PR China.

van Meurs, A. N. G., van den Berg, A., Venmans, A. A. M. & Zwabenburg, C. (1999). Embankment widening with the Gap-method. *Geotechnical Engineering for Transportation Infrastructure*, Barends, F. B. J., Lindenberg, J., Luger, H. J., Verruijt, A. & de Quelerij, L., Editors, CRC Press, Boca Raton, FL, USA, Vol. 2, pp. 1133–1138.

Zhang, J. H. (2007). *Study on the Deformational Behaviors and the Differential Settlement Controlling Standards of Widened Highway Embankment over Soft Soil*. PhD thesis, Southeast University, Nanjing, China (in Chinese).

The Editor welcomes discussion on all papers published in Geosynthetics International. Please email your contribution to discussion@geosynthetics-international.com by 15 April 2015.